Technology and Health Care 30 (2022) S413–S424
DOI 10.3233/THC-THC228038
IOS Press

Applying the N-isopropylacrylamide gel dosimeter to quantify dynamic dose effects: A feasibility study

Jung-Chang Sun[a,b], Bor-Tsung Hsieh[b], Chih-Ming Hsieh[c], Yuk-Wah Tsang[a,d,*] and Kai-Yuan Cheng[b,*]
[a]*Department of Radiation Oncology, Ditmanson Medical Foundation Chia-Yi Christian Hospital, Chiayi, Taiwan*
[b]*Department of Medical Imaging and Radiological Sciences, Central Taiwan University of Science and Technology, Taichung, Taiwan*
[c]*Department of Medical Imaging, Ditmanson Medical Foundation Chia-Yi Christian Hospital, Chiayi, Taiwan*
[d]*Department of Biomedical Engineering, Chung Yuan Christian University, Taoyuan, Taiwan*

Abstract.
BACKGROUND: The gel dosimeter is a chemical as well as a relative dosimeter.
OBJECTIVE: To evaluate the feasibility of using N-isopropylacrylamide (NIPAM) gel dosimeter to observe the dynamic dose effects and quantification of the respiration, and to help determine the safety margins.
METHODS: The NIPAM gel dosimeter combined with the dynamic phantom was used to simulate radiotherapy of lung or upper abdominal tumor. The field set to 4×5 cm^2, simulate respiratory rate of 4 sec/cycle, and motion range 2 cm. MRI was used for reading, and MATLAB was used for analysis. The 3%/3 mm gamma passing rate $> 95\%$ was used as a clinical basis for evaluation.
RESULTS: The dynamic dose curve was compared with 4×5, 4×4, 4×3 cm^2 TPS, and gamma passing rates were 74.32%, 54.83%, 30.18%. Gamma mapping demonstrated that the highest dose region was similar to the result of the 4×4 cm^2 TPS. After appropriate selection and comparing that the $\geqslant 60\%$ part of the dose curve with TPS, the gamma passing rate was 96.49%.
CONCLUSIONS: Using the NIPAM gel dosimeter with dynamic phantom to simulate organ motion during respiration for dynamic dose measurement and quantified the dynamic dose effect is feasible. The results are consistent with clinical evaluation standards.

Keywords: NIPAM gel dosimeter, dynamic dose effects, MRI

1. Introduction

The gel dosimeter is a chemical as well as a relative dosimeter. The gel dosimeter is advantageous in that it has a potential to provide stereoscopic relative dose distribution; however, uncommon clinical

*Corresponding authors: Professor Kai-Yuan Cheng, Department of Medical Imaging and Radiological Sciences, Central Taiwan University of Science and Technology, Taichung City 406053, Taiwan. E-mail: kycheng@ctust.edu.tw. Yuk-Wah Tsang, Department of Radiation Oncology, Ditmanson Medical Foundation Chia-Yi Christian Hospital, Chiayi City 60002, Taiwan. Tel.: 5 2765041 ext 7383. E-mail: 03754@cych.org.tw.

application is its disadvantage [1].

In 2006, Senden et al. developed a gel dosimeter with the monomer being N-isopropylacrylamide (NIPAM) that managed the issue of monomer toxicity [2]. After exposing the gel dosimeter to irradiation, reading equipment can be used to acquire the image data to analyze the dose. Common reading equipment include magnetic resonance imaging (MRI) [3], optical computed tomography (OCT), and computed tomography (CT), among which, MRI has advantages of high resolution and contrast as well as disadvantages of being expensive and the concern of dose variation caused by increased temperature after prolonged scanning [4].

Previous studies rarely focused on dynamic dosimetry; most of them just used the dynamic phantom to simulate organ motion for dose measurement as a clinical reference. In 2006, Sidhu et al. used the dynamic phantom and film to evaluate differences in dose uniformity of breast cancer treatment plans, and found that using simulation of dynamic phantom could show dose differences between different treatment plans and gating therapy improved dose homogeneity [5]. In 2012, Turner et al. tried to use the dynamic phantom verification to reduce the inaccuracy in target volume caused by internal motion and found that the accuracy of lung cancer radiotherapy improved with prior evaluation and health education combined with reasonably expanded therapeutic target volume [6].

In 2015, Hsieh et al. proposed a dynamic dose measurement applied to the calibration tube. They found that the dynamic dose response was similar to the static, and the average sensitivity difference of fixed and movement NIPAM was 0.001 s-1/Gy [7]. NIPAM gel dosimeters have also been used in static measurement, such as the study by Yao et al. in 2019. The results confirm that NIPAM gel dosimeter can be used for dose measurement of modern radiation technology [8]. However, most studies assume that the target treatment area is fixed, or the measurement of the calibration tube, and does not study the dynamic dose effect caused by physiological movement.

In this study, the NIPAM gel dosimeter was used, along with the dynamic motion of self-developed reciprocating dynamic phantom simulated organs and a linear accelerator, to simulate radiotherapy for the lung or upper abdominal tumor. MRI was used for evaluating the reading, and MATLAB was used for data analysis to study the dose distribution and dynamic effects of simulated respiration and to compare treatment planning system (TPS) to determine whether the clinical evaluation indices met standards and quantification results.

2. Material and methods

2.1. Preparation of NIPAM polymer gel

The NIPAM gel dosimeter used in this study was provided by the laboratory of the Department of Medical Imaging and Radiological Sciences of Central Taiwan University of Science and Technology (Taichung, Taiwan). The components included deionized water 87%, gelatin (300 Bloom type A, Sigma-Aldrich) 5%, NIPAM (97%, Sigma-Aldrich) 5% as a monomer, bisacrylamide (BIS, Mreck) 3%, and Tetrakis Hydroxymethyl Phosphonium Chloride (THPC, TCI) 5 mM as a deoxidant. To prepare the NIPAM gel dosimeter, we first dissolved gelatin in ionized water and stirred the solution until the gelatin was completely dissolved and fully expanded; the solution was subsequently water heated to 45°C and NIPAM and BIS were added as vulcanization agents. Stirring continued until the components were completely mixed. THPC was added to the solution to remove oxygen and stirred until the THPC completely dissolved. The prepared gel dosimeter was wrapped with tin foil to avoid light-induced polymerization, placed in 4°C fridge for solidification, and exposed to irradiation within 24 hr after preparation.

Table 1
The cylindrical flask irradiation settings in this study

Parameter	Set value
Gantry angle (degrees)	0
Photon energy (MV)	6
Irradiation dose (Gy)	5
Dose rate (cGy/min)	500
SSD (cm)	95
SAD (cm)	100

2.2. Automatically controlled sliding table for respiratory simulations

An automatically controlled sliding table was used to simulate respiration. The simulator motor drove the turntable, which enabled the sliding table and tray to support the phantoms. The simulator enabled the gel dosimeter and phantom to slide in the anterior-posterior direction at a sliding range of 1–3 cm for a sliding period of 1–7 s. In 1992, Korin et al. used an MRI to measure the movement of the upper abdominal organs and found the diaphragmatic muscle had the largest moving range in the craniocaudal direction, with a 1.3 cm moving range for normal breath and 3.9 cm for deep breath [9]. In 2003, Bussels et al. used MRI and found significant craniocaudal movement of thoracic and abdominal organs because of respiration [10]. In this study, a self-developed reciprocating dynamic phantom was used to simulate organ movement in the body. This phantom drove the sliding table back and forth to simulate craniocaudal organ motion. We set an anterior-posterior sliding range of 2 cm and period of 4 s/cycle, which was consistent with the median value of a respiration conversion frequency of approximately 12–20 times/min as proposed by Korin et al. in 1992.

2.3. Gel irradiation

The irradiation procedure was divided into two parts in this study. Varian Clinic 21 iX (Varian Medical Systems, USA) was used as an irradiator, and gelatin was always used first as the base to prepare the calibration tube and gel dosimeter before irradiation. Then the CT simulator was used to acquire CT images, and Varian's Eclipse^{TM} therapeutic planning system was used to develop radiotherapy plans and estimate MU values. The first part was gel calibration tube irradiation. A calibration tube, 10 cm in length and 1.5 cm in diameter, was filled with NIPAM gel. The irradiation settings had a gantry angle of 0°C, photon energy of 6 MV, dose rate of 500 cGy/min, and field of 20×20 cm^2. The gel tube was placed in an acrylic phantom of $30 \times 30 \times 4$ cm (L × W × H) with a 1.5 cm round hole at the center of the side, and a 10 cm thick solid water phantom was place underneath for irradiation. A dose calibration curve was plotted using the following data: a source to surface distance (SSD) for irradiation of 95 cm; a source to axis distance (SAD) of 100 cm; and irradiation doses of 0, 1, 2, 5, 8, and 10 Gy. The second part was the irradiation of the gel dosimeter. A cylindrical flask, 14 cm in length and 10 cm in diameter, was filled with NIPAM gel and irradiated after the simulation of the reciprocating dynamic phantom was turned on. The irradiation settings had field of 4×5 cm^2, the parameters are shown in Table 1. The gel dosimeter was fixed on the reciprocating dynamic phantom, as shown in Fig. 1. Based on the estimated dynamic simulation prognostic image shown in Fig. 2, it can be estimated that under ideal conditions, the area with the most dose would be 4×3 cm^2, as shown by the gray area in Fig. 2. Thus, treatment plans of 4×4 cm^2 and 4×3 cm^2 were prepared for future comparison.

Table 2
MRI scan parameters in this study

Parameter	Set value
Repetition time (ms)	3,000
Echo time (ms)	22, 44, 66, 88, 110, 132, 154, 176, 198, 220, 242, 264, 286, 308, 330, 352
FOV (mm × mm)	240 × 240
Matrix size	512 × 512
Slice thickness (mm)	5
Gap (mm)	0.5

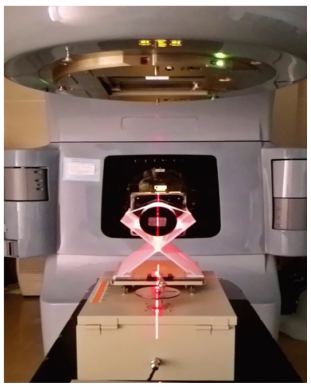

Fig. 1. Placing positions of the gel dosimeter and reciprocating phantom.

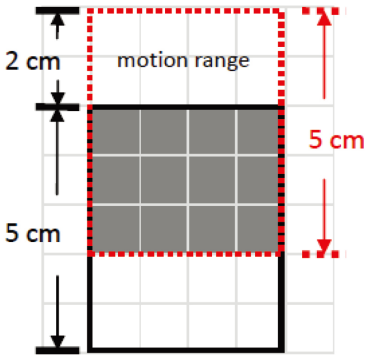

Fig. 2. Prognostic image of the reciprocating dynamic simulation. The simulated prognostic results showed that the gray area had the most doses.

2.4. MRI readout and image reconstruction

After irradiation, the gel dosimeter was first placed in the MRI examination room with temperature controlled between 22–24°C for 24 hours, allowing it to reach a balanced state with the ambient temperature of the examination room. The GE Healthcare-Brochure 1.5 T MR450w-with-GEM MRI machine; GEM head and neck unit with Geometry Embracing Method (GEM) coil; fast spin echo (FSE) T2WI imaging pulse sequence. MRI scan parameters as shown in Table 2. Images were taken 5 cm below the top of the container. After scanning, the images were sent to the GE advantage workstation 4.6 (AW 4.6) and PACS system for processing, then sent to computer and analyzed with MATLAB.

2.5. Gamma evaluation

After image reconstruction, the results measured using NIPAM gel dosimeters were compared with the TPS calculated data. The quantitative gamma evaluation proposed by Low et al. [11,12] was used for performance analysis. A basic consideration of dose distribution comparisons is to make them quantitative, yet allow the observer an efficient evaluation of the results. Dose distribution overlays provide a rapid overview of the two dose distributions. The dose-difference (DD) tool displays the numerical difference between two dose distributions. There are many striped regions that exceed 3% in the periphery of the dose distributions. The distance-to-agreement (DTA) tool was developed to provide the user with a measurement of the distance discrepancy between two dose distributions. The DTA becomes greater than 3 mm in the region where the dose discrepancy is 1%, except in the steep dose gradient region. The two dose distributions to be compared are assigned as the reference and evaluated distribution. The closest approach shortest distance of the reference distribution is identified as the gamma value. The gamma evaluation criteria, which are commonly used for clinical dose verification, were DTA = 3 mm and DD = 3%.

3. Results

3.1. Gamma passing rates

The gamma passing rates with gamma evaluation criteria of DTA = 3 mm and DD = 3% at TPS and measurement of MATLAB. On comparing 4×5 cm^2 TPS and the reading results, the gamma passing rate was determined as 74.32%. The objective of this study was to quantify the dynamic dose difference. The simulated moving pattern of the phantom was in the commonly used craniocaudal direction. Therefore, the ideal dose distribution under moving conditions was simulated first for evaluation. Based on the pre-simulation results, under the original field of 4×5 cm^2 moving back and forth with a dynamic range of 2 cm, the area with most doses was 4×3 cm^2, shown by the gray area in Fig. 2. However, the actual measured results showed that the 100% dose curve was close to 4×4 cm^2. Thus, a 4×4 cm^2 and 4×3 cm^2 TPS were further prepared to compare the reading results, and the gamma passing rates were found to be 54.83% and 30.18%, respectively.

3.2. Dose distribution and isodose line

Figure 3 shows the isodose line distribution of dynamic and TPS of 4×5 cm^2, 4×4 cm^2, and 4×3 cm^2. Figure 4 is the gamma map. Due to back-and-forth moving, the dose curve of isodose line distribution of dynamic showed an outward diffusion in the vertical direction, whereas there was no diffusion observed in the horizontal direction, and the 100% dose curve was close to 4×4 cm^2. As the gamma passing rate of 4×4 cm^2 TPS compared with the reading results was 54.83%, the estimated passing range should have been the $\geqslant 60\%$ region of the dose curve. On adjusting the ROI to make the comparing range close to 50% isodose line and comparing it with 4×4 cm^2 TPS, the gamma passing rates equaled 96.49%, as shown in Fig. 5.

3.3. Gamma map

Figure 6 shows the gamma map of 4×4 cm^2 TPS and MATLAB measurement after adjusting the ROI. The figure displays that the rejected area is mostly at the dose curve region of $< 60\%$, especially in the vertical direction. In this study, as the phantoms were moving back and forth, the rejected area in the vertical direction was greater than that in the horizontal direction, thus lowering the gamma passing rate.

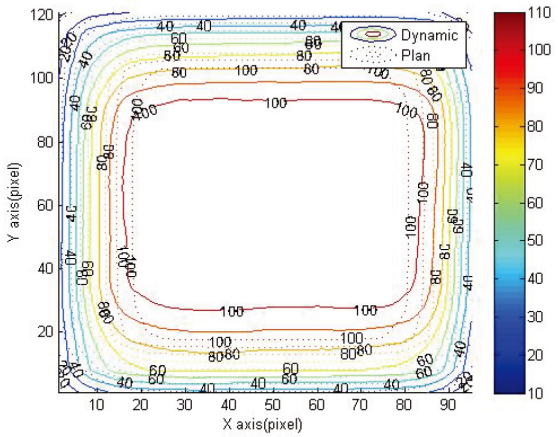

(a)

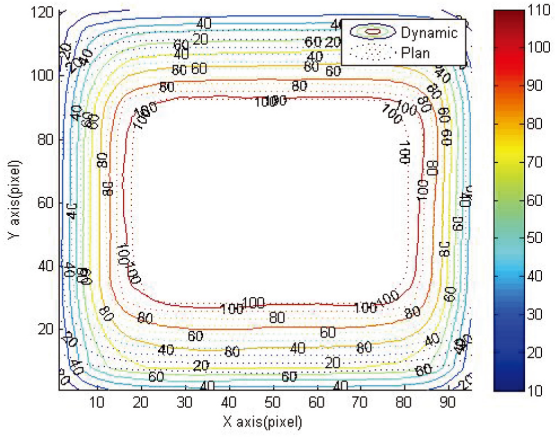

(b)

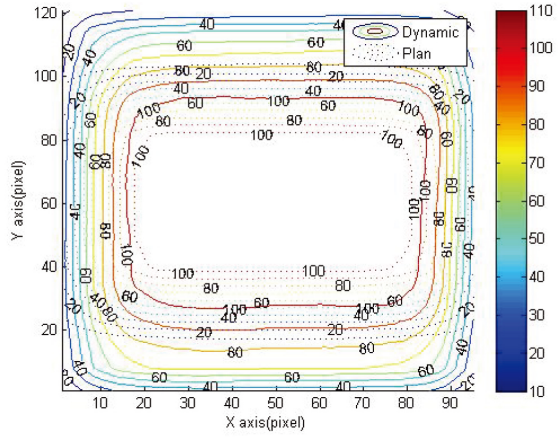

(c)

Fig. 3. Comparison between the reading results and TPS dose curve. From top to bottom: comparison results of (a) 4×5 cm^2, (b) 4×4 cm^2, (c) 4×3 cm^2.

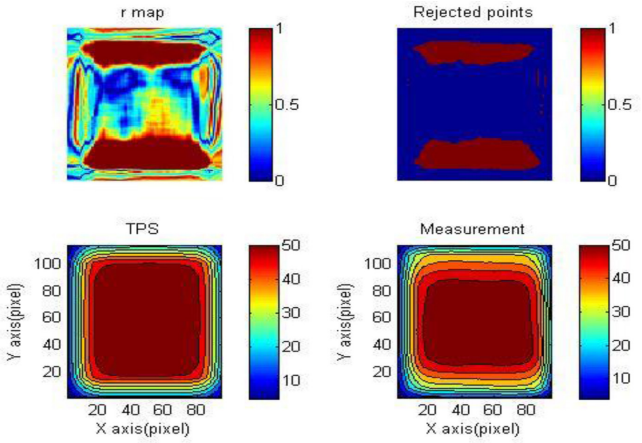

(a)

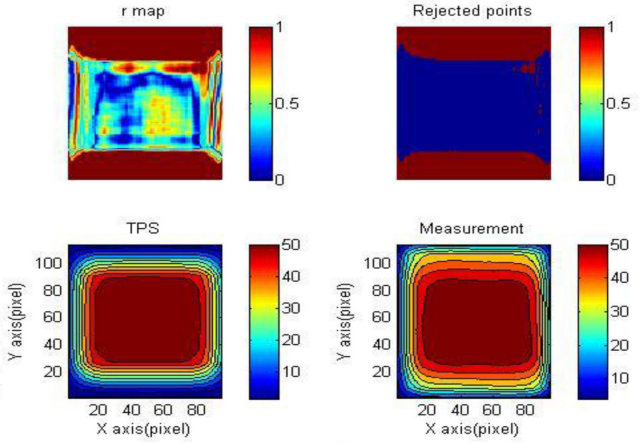

(b)

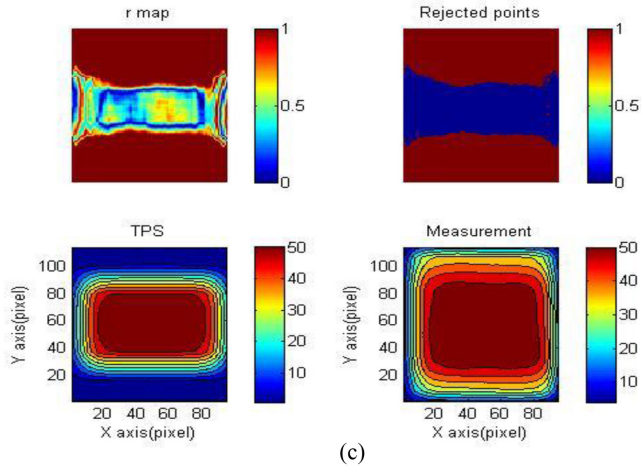

(c)

Fig. 4. Gamma map of reading results and TPS. From top to bottom: 3%/3 mm, gamma maps of (a) 4×5 cm^2, (b) 4×4 cm^2, (c) 4×3 cm^2.

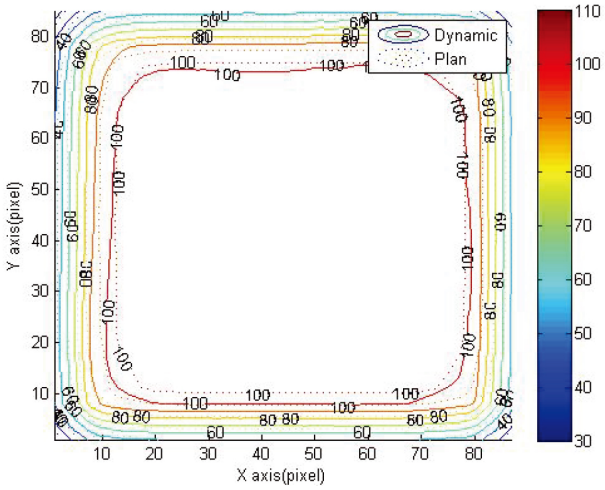

Fig. 5. Comparison between reading results and TPS 4 × 4 cm^2 ⩾ 60% dose curve.

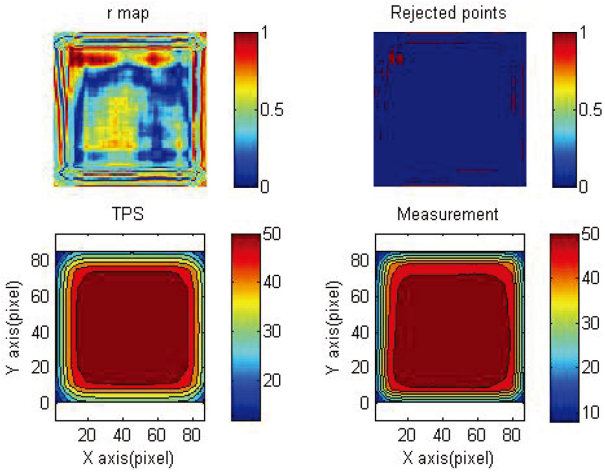

Fig. 6. 3%/3 mm gamma map of reading results and TPS 4 × 4 cm^2 ⩾ 60% dose curve.

4. Discussion

4.1. Quantification results of dynamic dose distribution during simulated respiration

The objective of this study was to evaluate the dose distribution dynamic effects and quantification outcomes of the NIPAM gel dosimeter when irradiated during the constant movement of the dynamic phantom. The evaluation method included obtaining reading results and comparing treatment plans and calculating whether 3%/3 mm gamma passing rates were ⩾ 95% to meet clinical evaluation standard. According to the results of this study, with a simulated respiratory rate of 4 sec/cycle and single breathing dynamic range of 2 cm, ⩾ 60% dose curve of a 4 × 5 cm^2 field was similar to that of a 4 × 4 cm^2 field. The 3%/3 mm gamma passing rate was 96.49%. This means that the dynamic range in the craniocaudal direction was 2 cm; the dynamic effect of ⩾ 60% dose curve distribution was 1 cm; and the affected area

was 50% of the dynamic range. A common clinical treatment for hepatoma, besides radiofrequency ablation (RFA), transarterial chemoembolization (TACE), and transarterial embolization (TAE), is stereotactic body radiation therapy (SBRT) [13]. The common screening criterion for hepatoma SBRT is single tumor $\leqslant 5$ cm; thus, the irradiation field in this study was set to 4×5 cm^2. The common evaluation method for modern radiotherapy is the gamma passing rate with a clinical evaluation standard of 3%/3 mm gamma passing rates being $\geqslant 95\%$. Therefore, the objective of this study was set to whether the analysis results met the clinical evaluation standards to determine whether the quantification results were reasonable; the results were proved to meet the clinical evaluation standards, and the quantification results were reasonable.

4.2. Improving overall accuracy of analysis results through internal calibration and independent calibration

The results of the study showed that under the dynamic simulated state, the 3%/3 mm gamma passing rate of the NIPAM gel dosimeter's analysis results comparing to the 4×5 cm^{2}TPS was 74.43%, which did not meet the clinical standard of 95%. However, in the ideal dose distribution of the estimated moving state, the 4×3 cm^2 area had the highest dose in the 4×5 cm^2 irradiation field in back-and-forth moving state, as shown by the gray area in Fig. 2. In addition, further examination found the similarity between the 100% dose curve and 4×4 cm^2 TPS. Thus, the 4×4 cm^2 and 4×3 cm^2 TPS were further prepared to compare with reading results, and the gamma passing rates were found to be 54.83% and 30.18%, respectively. Further examination found that even though the passing rate after comparing the reading results to 4×4 cm^2 TPS was lower than that of 4×5 cm^2 TPS, the passing rate of the high dose region was intact.

De Deene published a study on gel dosimeter reading results, suggesting that overall accuracy of analysis results can be improved through internal calibration and independent calibration in 2013. According to aforementioned results, the gamma passing rate for comparing reading results to 4×4 cm^2 TPS was 54.83%. It was speculated that all $\geqslant 50\%$ dose curves would meet clinical evaluation standards; thus, the ROI was adjusted to make a comparing range as close to a $\geqslant 50\%$ dose curve as possible. The results showed that reading results' $\geqslant 60\%$ region of dose curve was similar to the 4×4 cm^2 TPS. The 3%/3 mm gamma passing rate was 96.49%, which was higher than the clinical standard of 95%, and also higher than the 74.32% passing rate of comparing the reading results to 4×5 cm^2 TPS. This study demonstrated that the dynamic dose effect can be quantified; the quantification result was that the $\geqslant 60\%$ region of dose curve would be reduced, and the reduced area was 50% of the motion range.

4.3. Previous studies on dynamic dosimetry

Previous studies on dynamic gel dosimetry mainly focused on the coverage of dose volume histogram (DVH) and dynamic calibration tube measurement. In 2013, Thomas et al. used the PRESAGE gel dosimeter to examine organ movement interactions when administering radiotherapy, in which intensity modulated radiation therapy and RapidArc treatment plans were compared to reading results, and each target volume and DVH coverage were examined [14]. The results showed that there was similar DVH coverage between gross tumor volume (GTV) and clinical target volume (CTV), whereas there was greater difference in DVH coverage between internal target volume (ITV) and planning target volume (PTV). According to the author, if the leaf speed of a multileaf collimator, gantry rotation of the linear accelerator, and breathing period were all considered, the organ motion inaccuracy could be reduced. In this study, the NIPAM gel dosimeter was used to simulate the human body, and the common 3%/3 mm gamma passing

rate was used for comparison. It was found that GTV and CTV had similar coverage, whereas ITV and PTV had greater differences in coverage. In addition, by adjusting the selected comparing regions, it was found that the dynamic effect was 50% of the dynamic range. The region with dose curve $\geqslant 60\%$ had a gamma passing rate $> 95\%$ compared with TPS with dynamic effects deducted from the field, which had met the common clinical verification standard.

Hsieh et al. used the NIPAM gel dosimeter calibration tube combined with a respiration-simulating reciprocating phantom for dynamic and static irradiation, and used MRI reading for dose comparison in 2015. They found that the dose response of the calibration tube was consistent regardless of being dynamic or static. In the aforementioned study, the gel dosimeter calibration tube was placed in the reciprocating phantom during a respiration simulation, and the calibration tube was completely included in the irradiation field. Even in the dynamic state, the gel dosimeter would be within 100% dose distribution irradiation range; thus, the dynamic and static results were similar. This study confirmed that the NIPAM gel dosimeter can be used in measuring dynamic doses. To determine if it is applicable for clinical evaluation standards and dynamic dose effects, the dose curve distribution needs to be completely measured and compared with treatment plans to determine whether clinical evaluation standards are met. In our study, the NIPAM gel dosimeter was used to simulate the human body and combined with a reciprocating phantom to simulate craniocaudal motion during normal respiration. Dynamic simulated radiotherapy was administered, and MRI readings were used for dose measurement and dynamic effect evaluation as well as quantification result examination. The dynamic range effect was stimulated first to make comparisons between different treatment plans. It was found that through the adjustment of the selected range and comparison, the NIPAM gel dosimeter can be used in measuring dynamic doses, as well as in quantifying the dynamic dose effect. The quantification result was that the $\geqslant 60\%$ region of dose curve was reduced, and the reduced area was 50% of the dynamic range. The measuring results also met the clinical evaluation standards.

4.4. Suggestion on providing the definition of a tumor's safety margin

In 2011, Boda-Heggemann et al. used the dynamic phantom and CBCT to simulate image-guided radiotherapy for the lung tumor [15]. The results showed that comparing the results of simulating dynamic phantoms combined with breath-monitoring devices with clinical images, the accuracy of lung tumor treatment was increased. However, the breath-monitoring device was not commonly necessary.

Due to organ motion caused by physiological movement, radiotherapy of the lung and liver has relatively high uncertainty then head, neck, and brain. The technique of defining a tumor's safety margin is a key factor in developing radiotherapy plans. At present, the common defining methods include pre-treatment images, diagnostic information, suggestion from treatment guides, and physician's experience. In this study, the NIPAM gel dosimeter was used to simulate the human body combined with a reciprocating phantom to simulate craniocaudal motion during normal respiration to administer dynamic simulated radiotherapy, and MRI readings were used for dose measurement and dynamic effect evaluation as well as quantification result examination. The results showed that with a simulated respiratory rate of 4 sec/cycle and a breathing dynamic range of 2 cm, the $\geqslant 60\%$ dose curve of the 4×5 cm^2 field reduced to 4×4 cm^2, and the 3%/3 mm gamma passing rate was found to be 96.49%. Therefore, radiation oncologists can better define a tumor's safety margin by evaluating the patient's breathing dynamic range from pre-treatment images and diagnostic information, as well as the dynamic quantification results from this study, to reduce treatment uncertainty caused by organ motion and increase treatment accuracy.

4.5. Limitations and future developments

Although it has been confirmed in this study that NIPAM gel dosimeter can be used to evaluate the dynamic dose effect, the simulation is still different from the real physiological phenomenon to an extent as the movement of the dynamic phantom can only simulate a patient's craniocaudal motion. Moreover, single dynamic frequency and motion range were used in this study, which could be parameters that are too fixed when it comes to the frequency and range of real human respiration. Thus, studies on the technique of providing dynamic simulation that is more similar to the human body's real physiological phenomenon are warranted in the future. In addition, although the quantification result of the dynamic effect was confirmed in this study, for comparison results of unadjusted selecting range, the 74.32% passing rate from comparing the reading results to the 4×5 cm^2 TPS was still greater than the 54.83% passing rate from comparing the reading results to the 4×4 cm^2 TPS. In addition, although the study results confirmed that the dynamic effect causes the $\geqslant 60\%$ region of the original irradiation field's dose curve to shrink with the dynamic range, the $< 60\%$ region of the original irradiation field's dose curve did not completely shrink with the dynamic range as shown in Fig. 4a. As a result, when defining the safety margin of tumors, further exploration of whether a radiation oncologist should consider the 60% region of the original irradiation field's dose curve is warranted.

MRI was used as the reading instrument in this study. Although it is a common equipment in most hospitals, the reading not only requires setting and optimization of parameters but also needs subsequent reading analysis. It is not easy to write reading analysis programs for gel dosimetry, and the use of MRI, OCT, and CT all require writing corresponding reading analysis programs. Thus, how to establish a stable reading analysis program is an important factor to consider. Furthermore, although the NIPAM gel dosimeter has its advantage of displaying 3D dose distribution, it is not commonly used in clinical practice. Being a relative dosimeter, the gel dosimeter can not only be compared with the results of treatment plans but can also be compared with other common clinical dosimetric tools, such as films and ionization chambers, to increase the confidence level of the comparison results. This is another potential future field of study for interested researchers.

5. Conclusions

The gel dosimeter has a potential to provide stereoscopic relative dose distribution. In this study, the NIPAM gel dosimeter combined with the reciprocating dynamic phantom were used to simulate dose dynamic effect caused by organ motion during respiration. Through MRI reading and MATLAB reading analysis, the quantification of the dynamic effect was examined, and the common clinical standard of the 3%/3 mm gamma passing rate $> 95\%$ was used to determine whether the quantification result met the standards. The results showed that with a simulated respiratory rate of 4 sec/cycle and breathing dynamic range of 2 cm, the $\geqslant 60\%$ region of the original field's 4×5 cm^2 dose curve was reduced to 4×4 cm^2. The quantification result of the dynamic effect was that the $\geqslant 60\%$ region of dose curve was reduced, and the reduced area was 50% of the dynamic range. The 3%/3 mm gamma passing rate was 96.49%, which met the common clinical evaluation standard. This study proved that using the NIPAM gel dosimeter combined with the dynamic phantom to simulate organ motion during respiration for dynamic dose measurement is feasible, and with appropriate selecting and comparing analysis, the dynamic dose effect caused by organ motion can be quantified. In future studies, writing specific reading analysis programs for different reading equipment, adding other dynamic parameter settings, as well as comparing the findings with those of other common clinical dosimetric tools to provide more information to radiation oncologists

to determine the safety margin of tumors, which would reduce treatment uncertainty caused by organ motion and improve treatment accuracy, is recommended.

Acknowledgments

The authors immensely appreciate the financial support for this study provided by the Ditmanson Medical Foundation Chia-Yi Christian Hospital (Contract No. R107-14).

Conflict of interest

None to report.

References

[1] Azadbakht B, Adinehvand K. Investigation of the post time dependence of PAGAT gel dosimeter by electron beams using MRI technique. Res J Appl Sci Eng Technol. 2012; 4(3): 232-235.
[2] Senden RJ, Jean PD, McAuley KB, Schreiner LJ. Polymer gel dosimeters with reduced toxicity: a preliminary investigation of the NMR and optical dose response using different monomers. Phys Med Biol. 2006; 51: 3301-3314.
[3] Crescenti RA, Scheib SG, Schneider U, Gianolini S. Introducing gel dosimetry in a clinical environment: customization of polymer gel composition and magnetic resonance imaging parameters used for 3D dose verifications in radiosurgery and intensity modulated radiotherapy. Med Phys. 2007; 34(4): 1286-1297.
[4] De Deene YD, Vandecasteele J. On the reliability of 3D gel dosimetry. J Phys: Conf Ser. 2013; 444: 012015. doi: 10.1088/1742-6596/444/1/012015.
[5] Sidhu S, Sidhu NP, Lapointe C, Gryschuk G. The effects of intrafaction motion on dose Homogeneity in a breast phantom with physical wedges, enhanced dynamic wedges, and ssIMRT. Int J Radiat Oncol Biol Phys. 2006; 66(1): 64-75. doi: 10.1016/j.ijrobp.2006.03.045.
[6] Turner K, Cai J, Yin F, Zhang Y, Vergalasova I. A simple method to minimize uncertainty in ITV delineation: phantom verification. Med Phys. 2012; 39(6Part9): 3700-3701. doi: 10.1118/1.4735049.
[7] Hsieh C-M, Leung JH, Ng Y-B, et al. The feasibility assessment of radiation dose of movement 3D NIPAM gel by magnetic resonance imaging. Radiat Phys Chem. 2015; 116: 142-146. doi: 10.1016/j.radphyschem.2015.05.002.
[8] Yao C-H, Chang T-H, Lin C-C, et al. Three-dimensional Dose Verification of High-dose-rate (HDR) Flattening Filter Free (FFF) Radiation Therapy by using NIPAM Gel Dosimetry. JPS Conf. Proc. 2019; 24: 011025. doi: 10.7566/JPSCP.24.011025.
[9] Korin HW, Ehman RL, Riederer SJ, Felmlee JP, Grimm RC. Respiratory kinematics of the upper abdominal organs: a quantitative study. Magn Reson Med. 1992; 23(1): 172-178. doi: 10.1002/mrm.1910230118.
[10] Bussels B, Goethals L, Feron M, Bielen D, Dymarkowski S, Suetens P, et al. Respiration-induced movement of the upper abdominal organs: a pitfall for the three-dimensional conformal radiation treatment of pancreatic cancer. Radiother Oncol. 2003; 68(1): 74. doi: 10.1016/s0167-8140(03)00133-6.
[11] Low DA, Moran JM, Dempsey JF, Dong L, Oldham M. Dosimetry tools and techniques for IMRT. Med Phys. 2011; 38(3): 1313-1338. doi: 10.1118/1.3514120.
[12] Low DA, Harms WB, Mutic S, Purdy JA. A technique for the quantitative evaluation of dose distributions. Med Phys. 1998; 25(5): 656-661. doi: 10.1118/1.598248.
[13] Thomas HR, Feng M. Stereotactic body radiation therapy (SBRT) in hepatocellular carcinoma. Curr Hepatology Rep. 2021; 20(1): 12-22. doi: 10.1007/s11901-020-00559-1.
[14] Thomas A, Yan H, Oldham M, Juang T, Adamovics J, Yin FF. The effect of motion on IMRT – looking at interplay with 3D measurements. J Phys Conf Ser. 2013; 444: 012049. doi: 10.1088/1742-6596/444/1/012049.
[15] Boda-Heggemann J, Fleckenstein J, Lohr F, Wertz H, Nachit M, Blessing M, et al. Multiple Breath-Hold CBCT for online image guided radiotherapy of lung tumors: simulation with a dynamic phantom and first patient data. Radiother Oncol. 2011; 98(3): 309-316. doi: 10.1016/j.radonc.2011.01.019.